

Complexes [(P₂)Rh(hfacac)] as Model Compounds for the Fragment [(P₂)Rh] and as Highly Active Catalysts for CO₂ Hydrogenation: The Accessible Molecular Surface (AMS) Model as an Approach to Quantifying the Intrinsic Steric Properties of Chelating Ligands in Homogeneous Catalysis**

Klaus Angermund, Wolfgang Baumann, Eckhard Dinjus, Roland Fornika, Helmar Görls, Magnus Kessler, Carl Krüger, Walter Leitner,* and Frank Lutz

Abstract: The complexes [(P₂)Rh(hfacac)] **1** [P₂ = R₂P–(X)–PR₂] are introduced as model compounds for the investigation of the intrinsic steric properties of the [(P₂)Rh] fragment. The ligand exchange processes that occur during the syntheses of **1** from [(cod)Rh(hfacac)] and the appropriate chelating diphosphanes **3** were studied by variable-temperature multinuclear NMR spectroscopy. The molecular structures of eight examples of **1** with systematic structural variations in **3** were determined by X-ray crystallography. The

steric repulsion of the PR₂ groups within the chelating fragment was found to significantly influence the coordination geometry of [(P₂)Rh], depending on the nature and length of the backbone (X). A linear correlation between the P–Rh–P angles in the solid state and the ¹⁰³Rh

chemical shifts reveals a similar geometric situation in solution. A unique molecular modeling approach was developed to define the accessible molecular surface (AMS) of the rhodium center within the flexible [(P₂)Rh] fragment. The potential of this model for application in homogeneous catalysis was exemplified by the use of **1** as catalysts in a test reaction, the hydrogenation of CO₂ to formic acid. Complexes **1** were found to be the most active catalyst precursors for this process in organic solvents known to date.

Keywords: carbon dioxide activation · homogeneous catalysis · ligand effects · molecular modeling · rhodium

Introduction

The fragment [(P₂)Rh] (P₂ = chelating bidentate diphosphane of general formula R₂P–(X)–PR₂) plays a crucial role in a plethora of catalytic reactions, and the controlling influence of the chelating phosphane ligand on the activity and selectivity of such transformations is well documented.^[1] Understanding these effects on a molecular level is complicated by the fact that the fragment [(P₂)Rh] cannot be considered a rigid unit during catalysis, as it responds to steric and electronic interactions with other ligands. Surprisingly, only a few attempts have been made so far to elucidate the intrinsic influence of structural changes in

the phosphane moiety on the coordination geometry of the naked fragment [(P₂)Rh] and to correlate these changes with spectroscopic data, reactivity, or even catalytic properties.

Tolman's classical approach to describing structural effects in homogeneous catalysis has found wide application for monodentate phosphanes, but has severe limitations when applied to polydentate chelating ligands.^[2] One major drawback is the difficulty of taking into account the P–M–P angle (bite angle), which has arguably a strong influence on the reactivity of metal chelate complexes. Recent promising approaches to this problem include the experimental and theoretical work by Hofmann et al., who were able to rationalize aspects of the stoichiometric and catalytic chemistry of [(P₂)RhCl] fragments in terms of the P–Rh–P angle.^[3] Casey et al. have introduced the concept of *natural bite angle*, which proved to be a useful tool for the discussion of the relative stability of competing intermediates that lead to linear or branched aldehydes in rhodium-catalyzed hydroformylation.^[4]

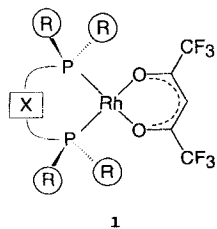
As part of our ongoing interest in rhodium-catalyzed hydrogenation of CO₂^[5–7] and in understanding the role of phosphane ligands in homogeneous catalysis,^[7, 8] we have systematically investigated the influence of structural changes in chelating ligands on the coordination geometry of the [(P₂)Rh] fragment and attempted to correlate the results with catalytic

[*] Priv.-Doz. Dr. W. Leitner, Dr. K. Angermund, Dipl.-Chem. M. Kessler, Prof. Dr. C. Krüger, Dr. F. Lutz
Max-Planck-Institut für Kohlenforschung, Kaiser-Wilhelm-Platz 1
45470 Mülheim/Ruhr (Germany)
Fax: Int. code + (208) 306-2980
e-mail: leitner@mpi-muelheim.mpg.de

Prof. Dr. E. Dinjus, Dr. R. Fornika, Dr. H. Görls
Arbeitsgruppe "CO₂-Chemie" der Max-Planck-Gesellschaft
an der Friedrich-Schiller-Universität Jena (Germany)

Dr. W. Baumann
Arbeitsgruppe "Komplekxkatalyse" der Max-Planck-Gesellschaft
an der Universität Rostock (Germany)

[**] Activation of Carbon Dioxide, Part 9. For Part 8, see ref. [10 d].



activity in the above-mentioned reaction. Here we give a full account on our approach, which is based on the synthesis of complexes $[(P_2)Rh(hfacac)]$ **1** (hfacac = hexafluoroacetylacetonate) as models for the naked $[(P_2)Rh]$ moiety and utilizes a combination of X-ray crystal structure analysis, ^{103}Rh NMR

spectroscopy, and molecular modeling. A key feature is the introduction of the concept of *accessible molecular surface* (AMS) for catalytically active transition metal centers,^[9] which represents a unique method for quantifying the intrinsic steric properties of a chelating ligand in homogeneous catalysis.

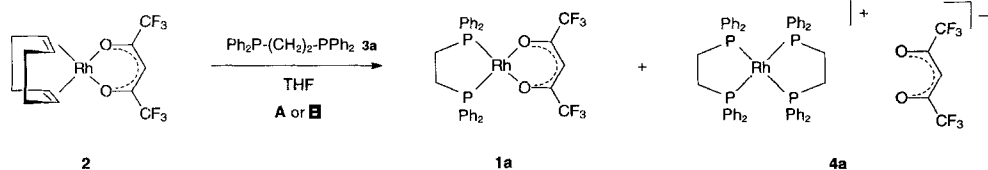
Complexes **1** appeared to be especially attractive for this investigation as we expected them to be readily accessible for a wide variety of ligands. Furthermore, little steric and electronic interaction between the phosphane moiety and the hfacac ligand was expected in these compounds. Finally, complexes **1** have been shown to be highly active catalysts for CO_2 hydrogenation,^[7a] and the corresponding mechanism is well understood.^[10]

Results and Discussion

Syntheses, structures, and catalytic properties of complexes $[(P_2)Rh(hfacac)]$ (**1**):

Synthesis of complexes 1: The replacement of labile olefin ligands in square-planar rhodium 1,3-diketone complexes by phosphane ligands appears to be a straightforward pathway to neutral complexes of general formula $[(P_2)Rh(1,3-diketone)]$.^[11] If, however, $[(cod)Rh(hfacac)]$ (**2**) is treated with one equivalent of the chelating phosphane $Ph_2P(CH_2)_2PPh_2$ **3a** at room temperature, the desired neutral complex **1a** is only obtained as the minor phosphorus-containing product and formation of the ionic complex $[(3a)_2Rh](hfacac)$ **4a** is preferred (Scheme 1).^[12] We found that the formation of **4a** can be suppressed if the phosphane is added slowly as a solution at low temperature and the reaction mixture is then allowed to warm to room temperature. A ratio of **1a** to **4a** of 23:1 was obtained when the addition was carried out at $-60^\circ C$, and **4a** was not detectable in the crude product by ^{31}P NMR when an initial reaction temperature of $-78^\circ C$ was used.

In these experiments, we observed that the typical dark red-brown color of the neutral complex **1a** started to appear only at temperatures above $-20^\circ C$. The above results indicate, however, that the product distribution is influenced by the temperature at which phosphane is added even well below this starting point. This discrepancy prompted us to investigate the substitu-

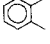
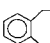
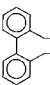
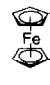
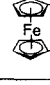


Scheme 1. Phosphorus-containing products obtained from the reaction of **2** with $Ph_2P(CH_2)_2PPh_2$ **3a**: A) Addition of **3a** as a solid in one portion at room temperature; B) dropwise addition of **3a** in THF at low temperature and slow warming to room temperature; see text for details.

tion process by variable-temperature NMR spectroscopy. The chelating phosphane $Me_2P(CH_2)_2PMe_2$ (**3d**) was chosen as the ligand in this study for practical reasons.

Phosphane **3d** undergoes an instantaneous reaction when it is injected as a neat liquid into a THF solution of **2** at 210 K, as shown by the absence of the signal for free phosphane in the ^{31}P NMR spectrum. Three new signals appear in the spectrum, all of them doublets owing to coupling of two chemically equivalent ^{31}P nuclei with a ^{103}Rh center (Figure 1). As suggested by the yellow color of the solution, the neutral complex **1d** is only present in very small amounts, indicated by a weak signal at $\delta = 54.4$ (cf. Table 1). The main phosphorus-containing

Table 1. Selected spectroscopic data [a] of complexes $[(P_2)Rh(hfacac)]$ **1**.

complex ligand 3	$1/$ -(X)-	R	δ (^{31}P)	$^1J_{RhP}$ (Hz)	δ (^{103}Rh)	δ (1H)	δ (^{19}F)	λ_{max} (nm)
a	$(CH_2)_2$	Ph	72.1	196	438	6.19	-76.1	400, 343, 272
b	$(CH_2)_2$	Cy	91.6	196	368	6.04	-76.5	425, 326, 274
c	$(CH_2)_2$	<i>i</i> Pr	101.2	195	323	6.05	-76.2	409, 326, 274
d	$(CH_2)_2$	Me	54.4	192	370	6.02	-76.5	n.d. [c]
e	$(CH_2)_3$	Ph	37.0	183	567	5.98	-76.3	272
f	$(CH_2)_4$	Ph	48.6	191	646	5.94	-77.2	399, 337, 272
g	$(CH_2)_4$	Cy	54.1	193	845	6.18	-76.2	431, 324, 270
h	$(CH_2)_5$	Ph	- [b]	-	-	-	-	-
i	$(CH_2)_6$	Ph	44.2	195	841	6.07	-76.1	n.d. [c]
k		Ph	74.3	195	450	6.05	-76.3	382, 273
l		Ph	42.3	193	696	5.84	-76.4	340, 272
m		Cy	47.6	197	932	6.03	n.d. [c]	n.d. [c]
n		Ph	52.1	205	825	5.93	-76.2	n.d. [c]
o		<i>i</i> Pr	64.5 [d]	205 [d]	1012	6.10	-76.3	429, 329, 271

[a] All measurements in THF solution. [b] Mixture of unidentified products. [c] n.d. = not determined. [d] These values replace those given in [7a].

product of the reaction of **2** with **3d** at 210 K is characterized by a resonance at $\delta = 38.3$ ($J = 145$ Hz). These values are typical for cationic olefin complexes $[(P_2)Rh(cod)]^+$, and the product was identified as the cation $[(3d)Rh(cod)]^+$ (**5d**⁺) by comparison of its 1H , ^{13}C , and ^{31}P NMR data with those of the complex $[(3d)Rh(cod)][CF_3SO_3]$ synthesized independently.^[13]

The doublet centered at $\delta = 36.8$ is readily assigned to the cation $[(3d)_2Rh]^+$ ($4d^+$) by comparison with literature data.^[14]

Figure 1 illustrates the changes in the distribution of the phosphorus-containing products on warming the reaction mixture

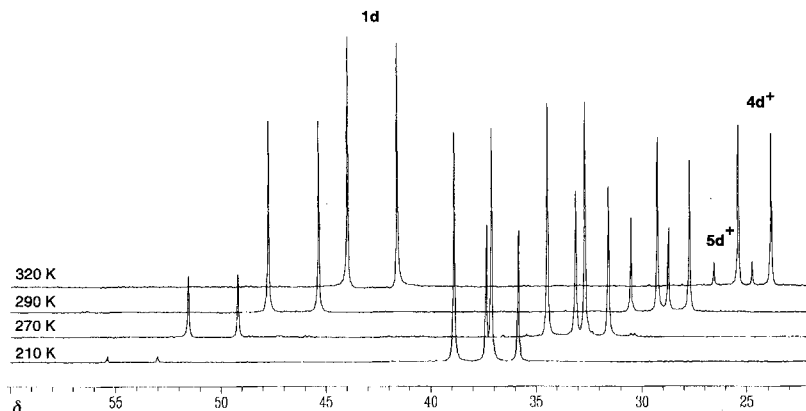
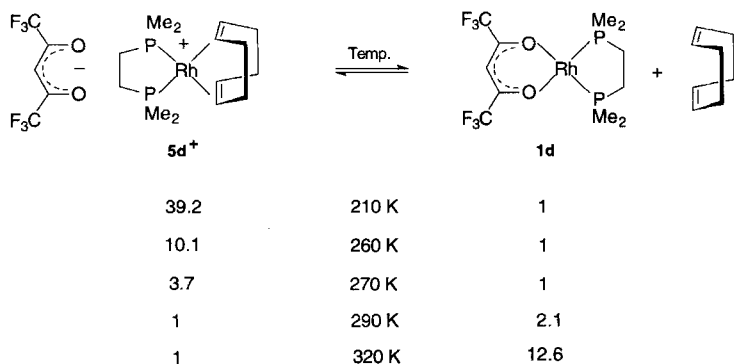


Figure 1. ^{31}P NMR spectra of the reaction mixture resulting from addition of neat $Me_2P(CH_2)_2PMe_2$ **3d** to a $[D_6]$ THF solution of **2** at 210 K and subsequent warming to 320 K.

stepwise to 320 K. The relative ratio of $4d^+$ to the sum of **1d** and $5d^+$ remains constant over the whole temperature range. The cationic olefin complex $5d^+$ is slowly converted to neutral **1d**, which becomes the major component above 280 K (Scheme 2).



Scheme 2. Changes in the ratio of complexes $5d^+$ and **1d** upon gradual warming of the reaction mixture obtained from addition of $Me_2P(CH_2)_2PMe_2$ **3d** to **2** in $[D_6]$ THF at 210 K.

The process is partly reversible, as demonstrated by gradually cooling the mixture from 320 to 240 K. The signals assigned to $5d^+$ grow again, although more slowly than they disappeared during warming.

The low-field region of the 1H NMR spectrum (Figure 2) of the reaction mixture at 260 K provides additional evidence for the equilibrium shown in Scheme 2. Integration of the methine proton signal of coordinated hfacac in **1d** at $\delta = 6.03$ and the olefinic protons of coordinated cod in $5d^+$ at $\delta = 5.18$ leads to a ratio of $5d^+$ and **1d** that is in reasonable agreement with that obtained from ^{31}P NMR. In addition, the presence of noncoordinated hfacac and cod is indicated by

resonances at $\delta = 5.56$ and 5.50, respectively. The chemical shift of the hfacac anion is somewhat temperature-dependent; the values vary from $\delta = 5.34$ at 210 K to $\delta = 5.72$ at 300 K.

An additional proton signal at $\delta = 4.28$ together with a correlated (2D $\{^{13}C, ^1H\}$ HETCOR experiment) doublet in the ^{13}C NMR spectrum at $\delta = 79.1$ [$^1J(RhC) = 14$ Hz] indicates the presence of a phosphane-free complex containing coordinated cod, since these values are identical to those of the starting material **2**. The presence of unreacted **2** is anticipated on the basis of the formation of the doubly phosphane-substituted cation $5d^+$ and the 1:1 stoichiometry of the reactants **2** and **3d**. However, the characteristic resonance at $\delta = 6.19$ for coordinated hfacac in **2** is not detectable in the 1H NMR spectrum at 260 K. This is probably due to a fast exchange process between free hfacac and **2**, indicated by the appearance of a very broad signal around $\delta = 6.2$ below 220 K. This exchange may also serve as an explanation for the temperature dependence of the signal for “free” hfacac described above.

The ^{19}F NMR spectra also indicate such an exchange process. At 260 K only two types of signal are present in the region typical for hfacac moieties. Taking into account the temperature dependence of the ^{19}F signals, the smaller sharp resonance at $\delta = -76.2$ can be assigned to coordinated hfacac of **1d**, while the larger, slightly broadened signal at $\delta = -76.7$ results from free hfacac and **2**. At 210 K this signal splits into two broad resonances at $\delta = -75.5$ and -76.9 .

Substitution reactions of square-planar [(1,3-diketonate)-Rh(olefin) $_2$] complexes have been studied in some detail over the last few years. It has been reported that the 1,3-diketonate ligand can be exchanged for other diketonate compounds^[15a] or substituted by nitrogen donor ligands.^[15b, c] On the other hand, the 1,3-diketonate moiety is regarded as a nonlabile spectator ligand in olefin exchange^[16] or olefin substitution by CO and phosphorus donor ligands.^[11] All these reactions were found to

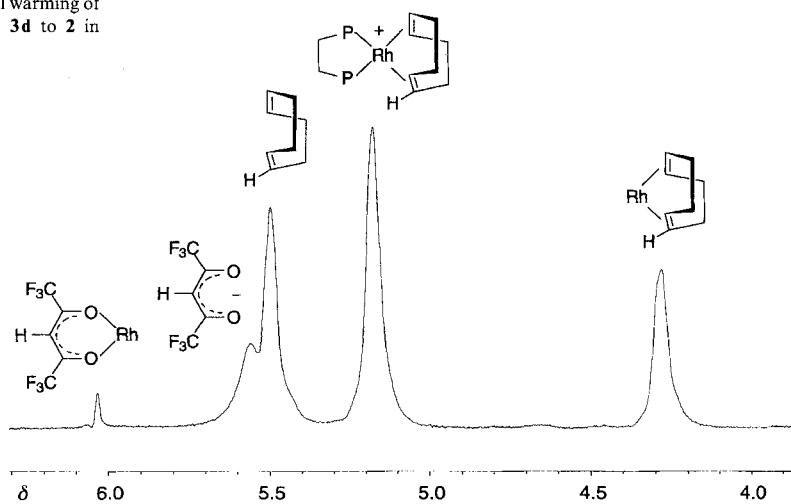


Figure 2. 1H NMR spectrum of the reaction mixture resulting from addition of neat $Me_2P(CH_2)_2PMe_2$ **3d** to a $[D_6]$ THF solution of **2** at 260 K.

proceed by associative pathways involving five-coordinate intermediates.^[11, 15, 16] These processes are of course reversible^[17] and our results clearly demonstrate that the "labile ligand" in **2** is therefore very much a matter of the actual reaction conditions. This unprecedented and somewhat unexpected observation should be kept in mind when catalysts are prepared in situ from complexes of type **2** and additional ligands.

The success of our synthetic procedure on a preparative scale can therefore be traced to the initial clean formation of **5d**⁺, which is subsequently converted to **1d**. Thus, following the procedure **B** outlined in Scheme 1, **2** was reacted with a variety of ligands R₂P(CH₂)_nPR₂ (*n* ≥ 2; R = Me, *i*Pr, Cy, Ph) **3a–i**, and the neutral complexes **1a–i** were obtained as red-brown glassy solids without formation of appreciable amounts of ionic complexes **4a–i** in all cases (Table 1). Only the phosphane Ph₂P(CH₂)₅PPh₂ **3h** failed to give an isolable complex **1h**. The synthesis was also successful for the preparation of complexes **1i–o**, in which the two phosphorus donor atoms are linked by backbone groups other than (CH₂)_n chains. Complexes **1a–o** were crystallized from diisopropyl ether or acetone and fully characterized by NMR, UV, and mass spectroscopy (Table 1 and supplementary material). X-ray crystal structure analyses (see section on solid-state structures of **1a–g** and **1o**) and elemental analyses were carried out for selected examples.

Spectroscopic properties of complexes 1a–o: The compounds **1a–o** exhibit typical spectroscopic data for square-planar 1,3-diketonate complexes of rhodium.^[11, 15, 16] All complexes **1a–o** show peaks for the molecular ion in the EI MS spectra. In addition, loss of the hfacac ligand is observed as a fairly general fragmentation pathway (see supplementary material). The ³¹P NMR resonances of **1a–o** are shifted downfield compared to the free ligands, whereby the magnitude of the downfield shift Δδ depends on the size of the chelate ring. The ring contribution Δ_R to this shift^[18] can be calculated for the chelating diphosphane ligands Ph₂P(CH₂)_nPPh₂ on the basis of Δδ = 62.7 for Ph₂PMe (δ = –26.1) and [(Ph₂PMe)Rh(hfacac)] (δ = 36.6). The Δ_R values are 20.2 for *n* = 2, –10.0 for *n* = 3, 0.2 for *n* = 4, and 3.1 for *n* = 6, and thus follow the typical pattern described by Garrou.^[18] The chemically equivalent ³¹P nuclei give rise to doublets with coupling constants ¹J(RhP) between 180 and 205 Hz, as expected for Rh(I) compounds with oxygen *trans* to phosphorus.^[19] The ¹⁹F and ¹H resonances of the hfacac ligand vary only slightly with the phosphane ligand. The same is true of the ¹³C NMR data (see supplementary material) of this fragment. Chemical shifts of insensitive transition-metal nuclei, particularly ¹⁰³Rh, are readily accessible in phosphane complexes by multiquantum-filtered two-dimensional ³¹P-detected NMR spectroscopy (so-called inverse two-dimensional shift correlation),^[20, 21] and a growing body of data is now available.^[20, 22] The values for **1a–o** are in the range expected for square-planar 1,3-diketonate complexes,^[16a, 20, 22c] but remarkable variations are observed on varying the ligand structure, with ¹⁰³Rh chemical shifts between δ = 323 and 1012. The exact δ values depend both on the groups R and on the nature of the backbone (X) (see below).

The UV spectra of complexes **1a–o** show three weak bands at approximately 400–430, 320–340, and 270 nm. The long-wave absorption is fairly broad and in some cases is not visible. Al-

though UV data of square-planar transition metal complexes containing 1,3-diketonate ligands do not necessarily give direct information on the d–d transitions,^[23] a linear correlation between δ(¹⁰³Rh), 1/ΔE_{d–d}, and λ_{max} has been observed in complexes [(olefin)₂Rh(1,3-diketonate)].^[16a] No correlation of this type is found for **1a–o**, as only variations of the groups R in **3a–o** have a significant impact on λ_{max}, while the bridging group X seems to be of minor importance.

Solid-state structures of 1a–g and 1o: Crystals suitable for X-ray crystal structure analysis were obtained for the starting material **2**^[24] and complexes **1a–g**^[7a] and **1o**.^[7a, 25] Selected bond lengths and angles are given in Figure 3 and Table 2. All com-

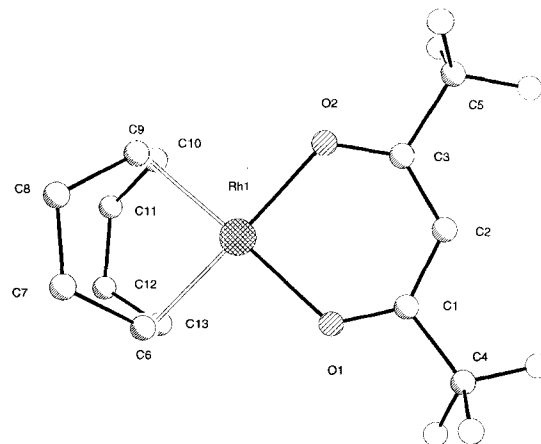


Figure 3. Molecular structure of [(cod)Rh(hfacac)] **2** as determined by single-crystal X-ray analysis. One of the two independent molecules in the unit cell is depicted. The fluorine atoms are in statistical disorder; only one of three arrangements is shown for clarity. Selected bond lengths [Å] and angles [°]: Rh–O 2.068(4), Rh–C 2.110(8), O–C 1.259(8), C=C 1.37(1), O–Rh–O 89.8(2), (C=C)–Rh–(C=C) 81.9(3).

Table 2. Selected structural features of complexes [(P₂)Rh(hfacac)] **1a–g** and **1o** obtained from X-ray crystal structure analyses.

Complex	Rh–P [Å] [a]	P–Rh–P [°]	Rh–O [Å] [a]	O–Rh–O [°]	C–O [Å] [a]	P–Rh–P/ O–Rh–O [°]
1a	2.191(1)	84.34(3)	2.100(2)	87.34(10)	1.253(4)	3.0
1b	2.193(1)	84.97(2)	2.101(2)	87.30(7)	1.250(3)	7.6
1c [b]	2.182(2)	86.01(7)	2.089(4)	87.5(2)	1.246(8)	4.9
1c' [b]	2.184(2)	86.15(8)	2.096(4)	87.5(2)	1.253(7)	2.1
1d	2.176(1)	85.08(5)	2.097(2)	88.5(2)	1.240(5)	0
1e	2.194(2)	90.77(6)	2.097(4)	86.8(1)	1.248(7)	3.8
1f	2.206(1)	93.08(3)	2.094(2)	86.95(8)	1.256(4)	1.1
1g	2.224(2)	98.93(6)	2.087(4)	87.7(2)	1.262(7)	5.1
1o [c]	2.228(1)	99.95(3)	2.088(2)	87.41(8)	1.254(3)	8.4

[a] The mean value of the two distances is given; the difference is less than 0.01 Å in all cases.

[b] Two independent molecules in the unit cell that differ in the ring puckering of the five-membered chelate. [c] Ref. [25].

though UV data of square-planar transition metal complexes containing 1,3-diketonate ligands do not necessarily give direct information on the d–d transitions,^[23] a linear correlation between δ(¹⁰³Rh), 1/ΔE_{d–d}, and λ_{max} has been observed in complexes [(olefin)₂Rh(1,3-diketonate)].^[16a] No correlation of this type is found for **1a–o**, as only variations of the groups R in **3a–o** have a significant impact on λ_{max}, while the bridging group X seems to be of minor importance.

The starting material **2** crystallizes in an orthorhombic system (space group *Pbca*). The 16-electron species **2** exhibits an ideal

square-planar coordination of rhodium by two C=C double bonds from cod and two oxygen atoms from hfacac (Figure 3). The first coordination sphere is almost identical to that observed in related complexes $[(\text{cod})\text{Rh}\{\text{RC}(\text{O})\text{CHC}(\text{O})\text{R}'\}]$ with $\text{R} = \text{R}' = \text{H}$ ^[26] or $\text{R} = \text{H}$ and $\text{R}' = \text{CF}_3$.^[11d] The observed C=C bond lengths do not allow the discussion of different back-bonding^[16a] for this series of complexes within experimental error.

The replacement of the cod ligand in **2** by a chelating phosphane results in a slightly elongated Rh–O bond and a somewhat compressed O–Rh–O angle, as illustrated by the molecular structure of complex **1d** in Figure 4 and further outlined in

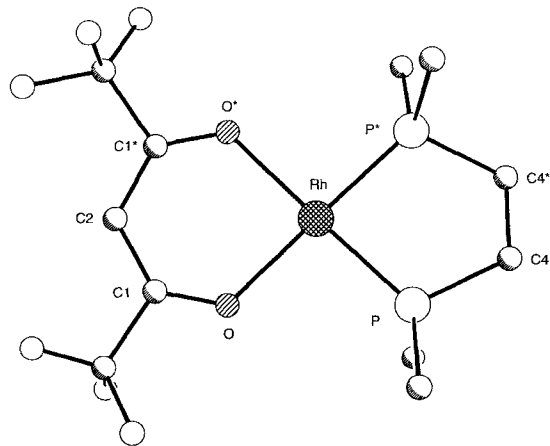


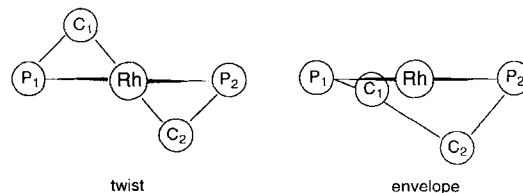
Figure 4. Molecular structure of $[(\mathbf{3d})\text{Rh}(\text{hfacac})]$ **1d** as determined by single-crystal X-ray analysis. The fluorine atoms are in statistical disorder; only one of three arrangements is shown for clarity. For selected bond lengths and angles, see Table 2.

Table 2. Within the series of phosphane complexes **1**, however, the coordination geometry of the hfacac moiety remains remarkably constant; mean values of 2.094(7) Å and 87.4(5)° are observed for the Rh–O distance and the O–Rh–O angle. Thus, the O–Rh–O angles in complexes **1a** and **1f** are almost identical [87.34(10) and 86.95(8)°], whereas the P–Rh–P angle increases from 84.34(3) to 93.08(3)°. The different basicities of the PR_2 groups in **1a–d** are not reflected in the Rh–O or C=O bond lengths.

Furthermore, the complexes show only very small deviations from an ideal square-planar arrangement, whereas considerable distortions are observed when steric interactions between PR_2 groups and other ligands such as cod or additional phosphanes occur in four-coordinate rhodium complexes.^[27] These constant features in the coordination geometry of complexes **1** regardless of variations in the phosphane ligand indicate that the hfacac moiety hardly interferes with the phosphane ligand. Thus changes in the coordination geometry of the $[(\text{P}_2)\text{Rh}]$ fragment can be considered to reflect the *intrinsic steric properties* of the chelating phosphane ligand.^[28]

The five-membered chelate rings of fragments $[\{\text{R}_2\text{P}(\text{CH}_2)_2\text{-PR}_2\}\text{Rh}]$ in the solid-state structures of **1a–d** can be classified into two types of arrangement:^[29] a twist conformation (**1d**, **1c**), and an envelope conformation. In the latter, the carbon atom C1 in the backbone is located either slightly above (**1b**, **1c'**) or below (**1a**) the P–Rh–P plane. A Cremer and Pople anal-

ysis^[30,31] of the structural data of 29 compounds containing 46 chelate rings formed with ligands **1a–d** on rhodium found in the Cambridge Structure Database^[32] revealed no systematic preference for either type of conformation depending on the groups R; steric interactions with other ligands and packing effects obviously play a major role.



Apart from these conformational changes, the coordination geometry shows very little variation throughout the range of complexes **1a–d** bearing five-membered chelate rings at the metal center. The Rh–P bond lengths and P–Rh–P angles do not reflect the changes of R in these complexes to a large extent. Using simple electronic arguments, one would expect that more basic trialkyl phosphorus ligands should exhibit shorter Rh–P distances than the bisaryl congeners. A significant shortening is, however, only observed for the sterically least demanding ligand **3d**. The Rh–P distances in **1a** and **1b** are identical within experimental error.

If the backbone chain is elongated with identical groups R at the phosphorus atom, the expected increase in the P–Rh–P angle is observed, as illustrated by **1a** (84.3°), **1e** (90.8°) and **1f** (93.1°). In contrast to five-membered chelates, the replacement of phenyl by cyclohexyl in $\text{R}_2\text{P}(\text{CH}_2)_4\text{PR}_2$ results not only in conformational changes, but also in a considerable increase of the P–Rh–P angle from 93.1 (**1f**, boat) to 98.9° (**1g**, twisted boat). This is accompanied by an increase in the Rh–P distance, contrary to what would be expected if the structure was dominated by phosphane basicity. Comparison of the couples **1a/b** and **1f/g** illustrates how the substitution of phenyl by cyclohexyl—groups which are identical in terms of classical ligand parameters such as electronic properties and steric bulk—may lead to considerably different effects on the overall geometry of the P_2Rh fragment.

These data lead to the conclusion that steric repulsion of the two R_2P groups within the chelate fragment has a significant influence on the P–Rh–P angle in fragments $[(\text{P}_2)\text{Rh}]$.^[33] A $(\text{CH}_2)_2$ bridge acts as a rather rigid “spring” and does not allow variation of the P–Rh–P angle. The incorporation of more than two CH_2 groups in the backbone allows larger and more variable angles^[4] and the two PR_2 groups can more readily increase their separation. The ferrocenyl bridge in **1o** naturally provides a wider spacer and may also offer some flexibility in the P–Rh–P angle, although this differs from the torsion modes in alkyl chains.^[34] In line with these considerations, a linear correlation ($r = 0.943$) is observed between the Rh–P distances and the P–Rh–P angles in structurally characterized complexes of type **1**, as shown in Figure 5. An alternative mode of increasing the P–Rh–P angle by stronger attraction of the Rh atom into the chelate ring through stronger Rh–P bonds would result in a simultaneous shortening of the P–Rh distance.

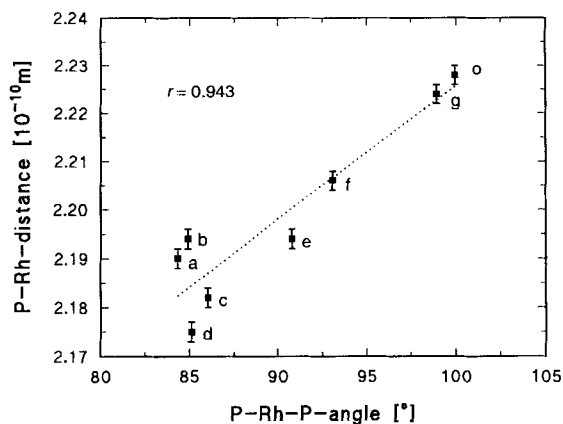


Figure 5. Correlation between the P-Rh-P angles and the P-Rh distances as determined from solid-state structures of complexes $[(P_2)Rh(hfacac)]$ **1a–g** and **1o**.

Complexes 1 as catalysts for CO₂ hydrogenation: Complexes **1a–o** are excellent catalysts for the hydrogenation of CO₂ to formic acid in dipolar nonprotic solvent systems [Eq. (1); DMSO/NEt₃ 5:1, $T = 298$ K, $p = 40$ bar] and maximum turnover numbers (total moles of HCOOH per mole of Rh, TON) of over 3000 have been reported.^[7a, 10d] Here, we wish to concentrate on the changes in the rate (turnover frequency, TOF) of formic acid production (Figure 6) observed upon

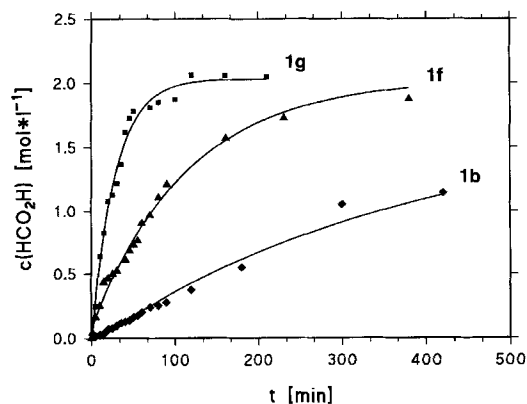
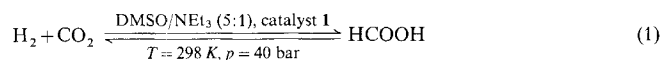


Figure 6. Increase of formic acid concentration during catalytic hydrogenation of CO₂ with catalysts $[(P_2)Rh(hfacac)]$ **1b**, **1f**, and **1g** (2.5×10^{-3} mol L⁻¹) in DMSO/NEt₃ (5:1) at 40 bar total pressure H₂/CO₂ (1:1) and 25°C.

structural changes within the chelating phosphane fragment in complexes of type **1**. These changes can be utilized to quantify the ligand effects on the catalytic properties of the rhodium centers.



The initial rates of reaction are obtained by linear regression of the early part (<10% of equilibrium concentration) of the concentration/time profiles as described in detail elsewhere.^[10d] They are readily converted to maximum TOFs by taking into account the given rhodium concentration. TOF values obtained under identical reaction conditions can then be used directly to compare the activities for complexes **1**. The characteristic catalytic data for selected complexes **1** are listed in Table 3.

Table 3. Characteristic catalytic data for complexes of $[(P_2)Rh(hfacac)]$ **1** and calculated structural features for the corresponding fragments $[(P_2)Rh]$.

complex 1 / ligand 3	-(X)-	R	TOF (h ⁻¹)	P-Rh-P (°) [a]	P-Rh-P (°) [b]	P-Rh (Å) [b]	AMS (Å ²) [c]
a	(CH ₂) ₂	Ph	170	86.9	83.26	2.171	7.578
b	(CH ₂) ₂	Cy	77	84.8	84.75	2.177	7.604
c	(CH ₂) ₂	<i>i</i> Pr	95	83.4	85.27	2.175	7.564
d	(CH ₂) ₂	Me	20	84.8	84.15	2.176	14.007
e	(CH ₂) ₃	Ph	300	90.9	88.79	2.182	5.704
f	(CH ₂) ₄	Ph	565	93.4	91.13	2.195	4.654
g	(CH ₂) ₄	Cy	1335	99.6	97.94	2.221	4.175
i	(CH ₂) ₆	Ph	– [d]	99.5	104.24	2.182	4.663
k		Ph	182	87.3	87.48	2.185	9.567
l		Ph	162	95.0	92.39	2.196	6.784
m		Cy	n.d. [e]	102.3	93.8	2.214	6.39
n		Ph	n.d. [e]	99.0	93.85	2.213	4.356
o		<i>i</i> Pr	687	104.8	99.48	2.235	4.493

[a] From $\delta(^{103}Rh)$ according to Equation (3). [b] From molecular modeling [9]. [c] AMS = accessible molecular surface; see text for details. [d] Rapid deactivation during the early stage of catalysis. [e] n.d. = not determined.

All complexes **1** tested as catalysts for CO₂ hydrogenation started the reaction with maximum rate from the beginning, since the catalytic species is formed directly under the given conditions.^[10c, d] The observed changes in catalytic activity can thus be considered intrinsic ligand effects for the $[(P_2)Rh]$ fragment, in contrast to the situation encountered with in situ catalysts, where the influence of the ligand on the formation of the active species may interfere with effects on the active center during catalysis.^[7b]

One might argue that ring opening of the $[(P_2)Rh]$ fragment could also play a role in defining the catalytic activity, either by deactivation through formation of oligomeric species^[35] or by activation through providing open coordination sites.^[36] In the case of deactivation, one would expect to observe nonlinear effects on the reaction rate upon varying the catalyst concentration. This has been excluded experimentally for **1e**^[10d] and **1f**. Furthermore, the equilibrium concentration of formic acid^[6b] was reached after appropriate reaction times and no deactivation of the catalysts **1** was observed over the course of the reaction, except with **1i**. The most likely pathway of catalyst deactivation in this case is formation of catalytically inactive Rh^{III} species by intramolecular C–H activation.^[37] Activation of the catalyst through P dissociation seems highly unlikely to be of major importance as only 16-e⁻ and 14-e⁻ species are involved in the catalytic cycle of CO₂ hydrogenation with complexes **1**,^[10d] so that enough open coordination sites are available without phosphane dissociation.

The TOF values observed with fragments $[(P_2)Rh]$ range from 20 h^{-1} for **1d** to 1335 h^{-1} for **1g**—a 67-fold increase in relative activity. Complexes with five-membered chelate rings **1a–d** and **1k** show TOF values not exceeding 200 h^{-1} . The complex **1g**, which contains a cyclohexyl-substituted seven-membered chelate ring, is the most active catalyst described so far for the hydrogenation of CO_2 to formic acid in organic solvents.^[5] In general, the activities of complexes **1** are considerably higher than those observed with in-situ catalysts formed from $\{(\text{cod})\text{Rh}(\mu\text{-Cl})_2\}_2$ and the same ligands.^[7b]

Correlation between structural properties, spectroscopic data and catalytic behavior of complexes $[(P_2)Rh(\text{hfacac})]$ (**1**):

The AMS model for homogenous catalysts: The results of the X-ray crystal analyses reveal that the coordination geometry at the rhodium center in $[(P_2)Rh]$ is largely determined by steric factors.^[28] In order to discuss catalytic properties on the basis of this finding, it is necessary to ensure that this situation also prevails in solution. A potentially sensitive probe for the changes in coordination geometry of metal complexes in solution is the chemical shift of the central metal atom, since the magnetic shielding and hence the chemical shift of a transition-metal nucleus is mainly determined by the paramagnetic contribution σ_p in the Ramsey model [Eq. (2)].^[20, 38] Changes in the coordination geometry are related to all parameters determining σ_p , whereas electronic changes can be expected to influence mainly ΔE_{d-d} .

$$\sigma = \sigma_d + \sigma_p = -A\rho_{\text{electrons}} + \frac{B\langle r_{nd}^{-3} \rangle D_i}{\Delta E_{d-d}} \quad (2)$$

Dominance of steric over electronic effects has been observed for olefin complexes of rhodium that contain monodentate^[20c, 22f] and bidentate^[22a, f, i] phosphane ligands. In the case of complexes **1** with P–Rh–P angles larger than 80° ,^[39] the direct linear correlation between the P–Rh–P angles obtained from X-ray analyses and $\delta(^{103}\text{Rh})$ strongly suggests that the coordination geometry is also the dominant factor determining the ^{103}Rh chemical shifts in complexes **1a–o** (Figure 7). A mathematical expression of the correlation ($r = 0.970$) is given in Equation (3). The P–Rh–P angles calculated according to Equation (3) for complexes of type **1** where no X-ray data are avail-

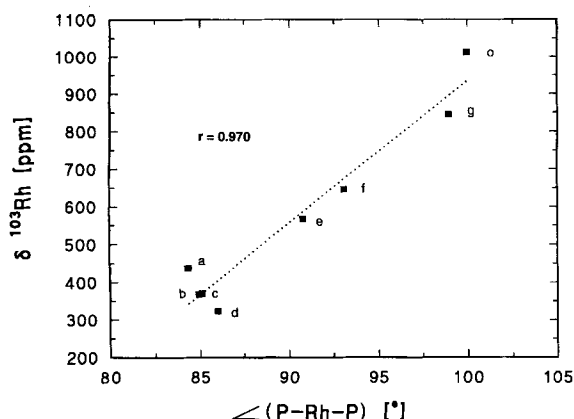


Figure 7. Correlation between P–Rh–P angles as obtained from X-ray crystal structure analyses and ^{103}Rh NMR shifts in complexes $[(P_2)Rh(\text{hfacac})]$ **1a–g** and **1o**.

able are in reasonable agreement with angles predicted from molecular mechanics, except for complex **1m** (Table 3).

$$\delta(^{103}\text{Rh}) = -2361.5 + 32.2 \times \angle(\text{PRhP}) \quad (3)$$

The chemical shifts of Group 9 transition metals have been successfully correlated to rates and selectivities of stoichiometric^[16a, 40] and catalytic^[22b, 41] reactions, whereby mostly direct electronic interactions were used to explain the observed relationships. Based on the relationship between $\delta(^{103}\text{Rh})$, P–Rh–P angle, and catalytic activity observed for complexes **1a–g** and **1o**, we have suggested that both the size of the P–Ph–P angle and the internal flexibility of the chelate ring are of major importance for the catalytic behavior of complexes **1** in CO_2 hydrogenation.^[7a]

This view is now further supported by the catalytic activities observed with **1k** and **1l**, in which a relatively rigid phenyl ring is incorporated in the $(\text{CH}_2)_n$ backbone of **1a** and **1f**, respectively. Complex **1k** shows a catalytic activity similar to **1a** as expected from the fact that both ligands **3a** and **3k** adopt similar P–Rh–P angles and five-membered chelate rings in general show only limited geometrical flexibility (see above). The P–Rh–P angles in **1f** and **1l** are also very similar, but the perturbation of the possible internal movements of the flexible $(\text{CH}_2)_4$ bridge leads to a sharp decrease of catalytic activity in **1l** compared to **1f**.

In search for a model that could give a concise description of all these sterically relevant parameters, the concept of the accessible molecular surface (AMS)^[9] has been developed for the present system. The basic idea of this model is to combine the simplicity and clarity of a purely steric model with the computational ability to describe the steric properties in a more general, conformationally dependent form. The AMS analysis for a homogeneous transition metal catalyst in general consists of three basic steps: 1) exploration of the conformational space of the active fragment, 2) superposition of selected relevant structures, and 3) analysis of the resulting “pseudo-dynamic” structure. Ultimately, correlations between the data obtained in step (3) and activities or selectivities in catalytic reactions may be established. Such correlations, although purely empirical in the first place, may then help to rationalize the observed ligand effects and lead to the development of more efficient catalysts.

In the present case, molecular mechanics were used to explore the conformational space of complexes **1**, since extended force-field parameters could be extracted from the X-ray data for **1a–g** and **1o** as a broad and reliable basis. Systematic search procedures based on an extended Tripos force field have been applied by using torsion angle increments of 10° for ring bonds and 30° for other single bonds. Maximum deviation from the ideal geometry of the ring-closure bond was 5° for valence angles and 0.25 \AA for bond lengths. Conformations were considered valid if the maximum overlap of van der Waals radii did not exceed 20%.

For example, this procedure led to 36 and 188 relevant conformations for **1d** and **1g**, respectively. These individual conformations were then superimposed (best fit of atom positions PRhP) to provide a “pseudo-dynamic” model of the ligand sphere as shown in Figure 8 for the fragments $[(P_2)Rh]$, with $P_2 = \mathbf{3d}$ and $\mathbf{3g}$ corresponding to the least active and most active catalyst precursors **1d** and **1g**.

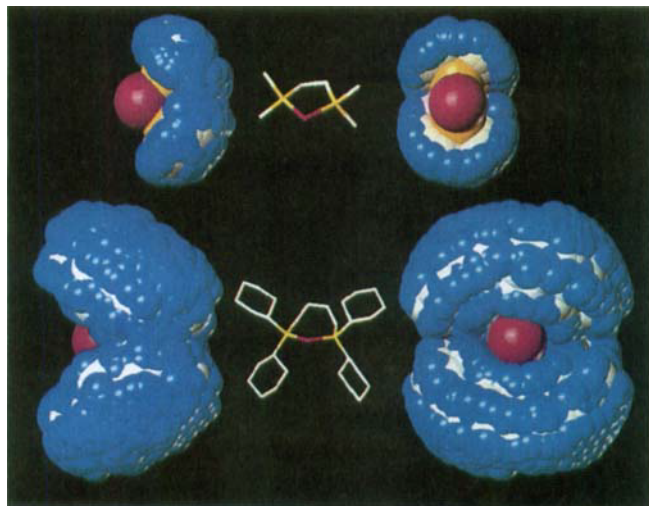


Figure 8. Front and side view of the van der Waals surface of a superposition of the results of a full conformational search^[9] for the fragments $[(P_2)Rh]$ with $P_2 = 3d$ (top) and $3g$ (bottom) corresponding to the least active and most active catalyst precursors $1d$ and $1g$. The colors represent positions of hydrogen (blue), carbon (white), phosphorus (yellow), and rhodium (magenta) atoms, respectively.

Figure 8 demonstrates how the shape and the size of the open cavity is determined not only by the P-Rh-P angle and the steric bulk of R, but also by the flexibility of the groups R at phosphorus and by possible internal movements within the chelate ring. The cavity thus reflects all relevant parameters for a description of the intrinsic steric properties of the $[(P_2)Rh]$ fragment. The obvious difference in the accessibility of the rhodium center within the cavity is readily quantified by AMS analysis. In the present case, a shape-independent value of the AMS was determined by calculating a “pseudo-solvent-accessible” surface (probe radius 1.4 Å), similar to a methodology known as the Connolly surface method used in biochemistry for the description of active centers in enzymes.^[9, 42] The ligand $3g$ yields the smallest AMS for the central metal atom, whereas $3d$ provides the most “accessible” rhodium center in the present series of ligands (Table 3).

Figure 9 displays a plot of the AMS of the rhodium center in the $[(P_2)Rh]$ fragment versus the TOF values observed for the

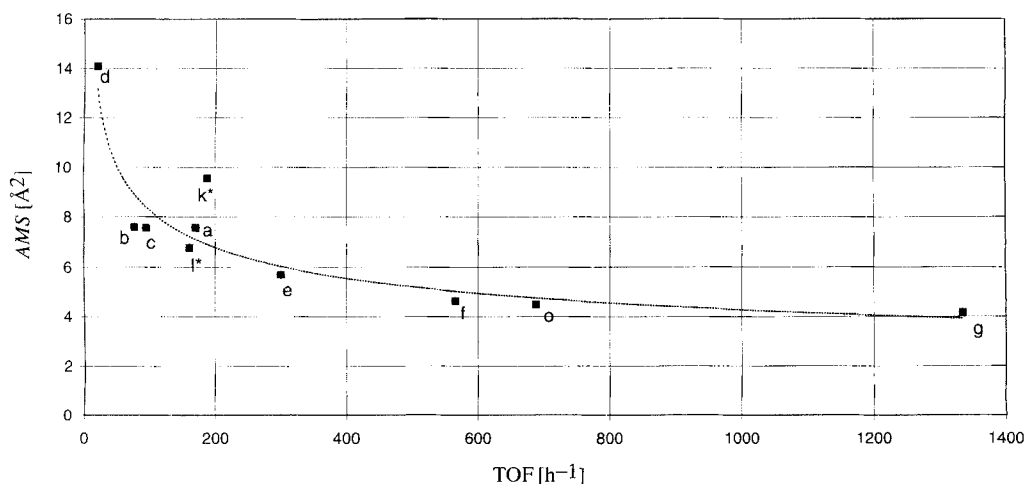


Figure 9. Correlation between TOF values observed with selected catalysts $[(P_2)Rh(hfacac)]$ **1** in the hydrogenation of CO_2 to formic acid and the AMS of the rhodium center of the corresponding fragments $[(P_2)Rh]$.

corresponding complexes **1** in CO_2 hydrogenation. Qualitatively, the activity of the catalysts increases strongly with decreasing accessibility of the metal center or, in other words, with an increasing shielding effect of the ligand. Most notably, the ligands **3i** and **3o**, whose activities are difficult to rationalize solely on the basis of the P-Rh-P angles in **1i** and **1o**, follow the same trend. Note that the fit curve is only for illustration and does not represent a mathematical analysis.

Of course, the observed empirical relation reflects a highly simplified model approach and does not necessarily imply any real physical events in the reaction solution. However, within a purely steric model,^[43, 44] one might predict that the fragment $[(3g)Rh]$ would be best suited for a catalytic cycle in which the coordination number decreases in the rate-limiting step, whereas $[(3d)Rh]$ is suitable for the inverse case. In this respect, the observed trend is consistent with experimental and theoretical studies on the mechanism of CO_2 hydrogenation to formic acid under the given conditions, which suggest the liberation of formic acid from the catalytic active center to regenerate the 14-e species $[(P_2)RhH]$ as the rate-limiting step of the catalytic cycle.^[10d] The beneficial effect of a ligand like **3g** for this reaction can thus be plausibly attributed to its ability to “push” the product away from the active center and at the same time to prevent the highly active intermediate $[(P_2)RhH]$ from undesired stabilization by addition of donor molecules such as solvent or amine, or by oligomerization.^[3, 45]

Conclusions

A general synthetic methodology for the preparation of complexes $[(P_2)Rh(hfacac)]$ (**1**; $P_2 = R_2P-(X)-PR_2$) has been developed and some unusual ligand exchange processes that occur during their formation have been elucidated. The complexes **1** were shown to be versatile model compounds for the investigation of intrinsic steric properties of chelating phosphane ligands, owing to a marginal electronic and steric interaction between the phosphane fragment and the hfacac ligand. The coordination geometry of the $[(P_2)Rh]$ fragment in the solid state and in solution was found to be significantly influenced by the steric

repulsion of the PR_2 groups within the chelate ring. This influence was shown to vary with the nature and length, or more precisely the rigidity, of the backbone (X). X-ray crystal structure data obtained upon systematic variation of R and (X) in complexes **1** were used as a basis for molecular modeling studies on the $[(P_2)Rh]$ fragment.

On the basis of these results, we were able to introduce the accessible molecular surface (AMS) model as a unique approach for the description of steric ligand

effects in homogeneous catalysis. Its use was demonstrated for the first time in the rhodium-catalyzed hydrogenation of CO₂ to formic acid with complexes **1** as the catalyst precursors. This concept may serve as a general approach to understanding ligand effects on activity and especially selectivity in processes that are mainly governed by steric interactions. The fact that not only the size but also the shape of the cavity of the active fragment can be analyzed by this methodology opens a whole range of possible applications, especially in stereoselective syntheses.

Experimental Section

General methodologies and materials: All reactions involving air- or moisture-sensitive materials were performed under argon by means of standard Schlenk techniques in dried and deoxygenated solvents. The complex [Rh(cod)(hfacac)] **2** was synthesized by the literature procedure.^[15c] With the exception of **3m** and **3o**, the ligands **3** were commercial products or prepared following known procedures.^[46]

NMR spectra were recorded in 5 mm tubes on a Bruker AC 200 spectrometer operating at 200.13, 50.29, 188.15, and 80.15 MHz for ¹H, ¹³C, ¹⁹F, and ³¹P. Chemical shifts δ are reported in ppm relative to external CFCl₃ for ¹⁹F, H₃PO₄ for ³¹P, and TMS for ¹H and ¹³C, using the solvent resonance as a secondary standard if possible. Coupling constants *J* are given in Hz. UV spectra were recorded on a Varian 2300 spectrophotometer in 1 mm cells at concentrations of approximately 1 mg mL⁻¹. Mass spectra were measured on a Finnigan MAT S50 Q710 with the EI-MS technique. Elemental analyses were carried out on a LECO CHNS 932 at the Laboratory of Organic Chemistry, Friedrich-Schiller-Universität Jena.

General method for the preparation of complexes [(P₂)Rh(hfacac)] (1a–o): One equivalent of the chelating phosphane **3a–o** in THF (15 mL) was added dropwise to a solution of **2** (300 mg, 0.72 mmol) in 15 mL THF at –78 °C. The reaction mixture was allowed to warm to room temperature and the volatiles were removed in vacuo. The glassy residues were dried under high vacuum for 24 h to yield quantitatively **1a–o** as red-brown powders containing varying amounts of THF, but less than 5% phosphorus-containing impurities according to NMR analysis. Analytically pure samples were obtained by crystallization from diisopropylether or acetone (**1b**). Characteristic spectroscopic data are given in Table 1; full details including MS and ¹³C NMR data are available as supplementary material from the authors.

Determination of $\delta(^{103}\text{Rh})$: The 2D(³¹P, ¹⁰³Rh{¹H}) spectra were recorded on a Bruker ARX 400 spectrometer (*B*₀ = 9.4 T) at ca. 298 K. The standard four-pulse HMQC sequence^[47] was performed twice with variation of the ¹⁰³Rh frequency offset and the *t*₁ increment to ensure that signals in the F1 dimension (¹⁰³Rh) were not folded. Typical conditions: 128 experiments in *t*₁, 4 or 8 scans each, 4 s relaxation delay, total experimental time ca. 40–80 min. The ¹⁰³Rh shifts are given relative to $\Xi(^{103}\text{Rh}) = 3.16 \text{ MHz}^{[20]}$ and were reproducible within 1 ppm.

Determination of the turnover frequencies TOF: A 200 mL stainless steel autoclave equipped with a glass liner, magnetic stirring bar and sampling device was evacuated and purged with argon three times. The reaction mixture, consisting of DMSO (20 mL), NEt₃ (4 mL) and 0.06 mmol of the appropriate complex **1** was transferred to the autoclave from a Schlenk tube with positive argon pressure through a teflon canula connected to the sampling system. The mixture was stirred under H₂ (20 atm) for 30 min, after which CO₂ was introduced up to a total pressure of 40 atm without stirring. The reaction was started by switching on the stirrer at a constant rate of 1000 rpm and small samples (ca 0.1 mL) were withdrawn at given time intervals. The formic acid concentration was determined by ¹H NMR spectroscopy^[10d]. Initial rates *v*₀ were obtained from linear regression of data points within the early stages of catalysis (< 10% of equilibrium concentration) and converted to TOF values according to Equation (4).

$$\text{TOF}(\text{I}) = \frac{v_0(\text{I})}{c(\text{I})} = \frac{v_0(\text{I})}{2.5 \times 10^{-3} \text{ mol L}^{-1}} \quad (4)$$

Acknowledgments: This work was supported by the Max Planck Society, the BMBF, and the Fonds der Chemischen Industrie. W. L. wishes to thank Prof. P. Jolly, Mülheim, for communicating unpublished results. The help of Dr. K. Seevogel, Mülheim, in collecting the UV data, and the preparative assistance of U. Beneke, Jena, are gratefully acknowledged. The ligands **3o** and **3m** were kindly provided by Dr. P. A. Chaloner, Brighton, and Prof. M. T. Reetz, Mülheim, respectively. Generous loans of chemicals were received from Degussa AG and Hoechst AG.

Received: September 23, 1996 [F 475]

- [1] a) *Comprehensive Organometallic Chemistry, Vol. 12*, (Eds.: E. W. Abel, F. G. A. Stone, G. Wilkinson) Pergamon, Oxford, 1995; b) R. H. Crabtree, *The Organometallic Chemistry of the Transition Metals*, 2nd ed., Wiley, New York, 1994; c) *Homogeneous Transition-Metal Catalyzed Reactions* (Eds.: W. R. Moser, D. W. Slocum), *Adv. Chem. Ser.* 1992, 230; d) *Applied Homogeneous Catalysis with Organometallic Compounds* (Eds.: B. Cornils, W. A. Herrmann), VCH, Weinheim, 1996.
- [2] C. A. Tolman, *Chem. Rev.* 1977, 77, 312.
- [3] a) P. Hofmann, C. Meier, U. Englert, M. U. Schmidt, *Chem. Ber.* 1992, 125, 353; b) P. Hofmann, C. Meier, W. Hiller, M. Heckel, J. Riede, M. U. Schmidt, *J. Organomet. Chem.* 1995, 490, 51.
- [4] a) C. P. Casey, G. T. Whiteker, *Isr. J. Chem.* 1990, 30, 299; b) C. P. Casey, G. T. Whiteker, M. G. Melville, L. M. Petrovich, J. A. Gavney, Jr., D. R. Powell, *J. Am. Chem. Soc.* 1992, 114, 5535; c) M. Kranenburg, Y. E. M. Van der Burgt, P. C. J. Kramer, P. W. N. M. Van Leeuwen, K. Goubike, J. Fraanje, *Organometallics* 1995, 14, 3081.
- [5] For recent reviews, see: a) P. G. Jessop, T. Ikariya, R. Noyori, *Chem. Rev.* 1995, 95, 259; b) W. Leitner, *Angew. Chem.* 1995, 107, 2391; *Angew. Chem. Int. Ed. Engl.* 1995, 34, 2207; c) W. Leitner, *Coord. Chem. Rev.* 1996, 153, 257.
- [6] a) E. Graf, W. Leitner, *J. Chem. Soc. Chem. Commun.* 1992, 623; b) W. Leitner, E. Dinjus, F. Gassner, *J. Organomet. Chem.* 1994, 475, 257; c) F. Gassner, W. Leitner, *J. Chem. Soc. Chem. Commun.* 1993, 1465.
- [7] a) R. Fornika, H. Görls, B. Seemann, W. Leitner, *J. Chem. Soc. Chem. Commun.* 1995, 1479; b) E. Graf, W. Leitner, *Chem. Ber.* 1996, 129, 91.
- [8] J. Bruckmann, C. Krüger, F. Lutz, *Z. Naturforsch.* 1995, 50B, 351.
- [9] Technical details of the molecular modeling approach will be published separately.
- [10] a) T. Burgemeister, F. Kastner, W. Leitner, *Angew. Chem.* 1993, 105, 781; *Angew. Chem. Int. Ed. Engl.* 1993, 32, 739; b) F. Hutschka, A. Dedieu, W. Leitner, *ibid.* 1995, 107, 1905 and 1995, 34, 1742; c) F. Gassner, H. Görls, E. Dinjus, W. Leitner, *Organometallics* 1996, 15, 2078; d) F. Hutschka, A. Dedieu, M. Eichberger, R. Fornika, W. Leitner, *J. Am. Chem. Soc.* 1997, in press.
- [11] For some related examples, see: a) D. M. Barlex, J. Hacker, R. D. W. Kemmit, *J. Organomet. Chem.* 1972, 43, 425; b) W. Partenheimer, E. F. Hoy, *J. Am. Chem. Soc.* 1973, 95, 2840; c) P. J. Fennis, H. M. Budzelaar, H. G. Frijns, A. G. Orpen, *J. Organomet. Chem.* 1990, 393, 287; d) Z. Duan, M. J. Hampden-Smith, E. N. Duesler, *Polyhedron* 1994, 13, 609.
- [12] A similar observation has been made in earlier studies [11c,d] but was not investigated in more detail.
- [13] J. M. Brown, P. L. Evans, A. P. James, *Org. Synth.* 1989, 68, 64.
- [14] T. B. Marder, I. D. Williams, *J. Chem. Soc. Chem. Commun.* 1987, 1478.
- [15] a) J. H. Potgieter, *J. Organomet. Chem.* 1989, 366, 369; b) J. G. Leipoldt, G. J. Lamprecht, E. C. Steynberg, *ibid.* 1990, 397, 239; c) J. G. Leipoldt, E. C. Grobler, *Trans. Met. Chem.* 1986, 11, 110.
- [16] a) B. Akermark, R. A. Blomberg, J. Glaser, L. Öhrström, S. Wahlberg, K. Wärnmark, K. Zetterberg, *J. Am. Chem. Soc.* 1994, 116, 3405; b) R. Cramer, *ibid.* 1964, 86, 217.
- [17] NMR spectra of a THF solution of **2** in the presence of excess cod did not reveal any indication of cod exchange [16] or formation of free hfacac over the temperature range 240–300 K. However, very small amounts of **2** could be detected and very slow appearance of **4d** could be observed after several days if cod was added to **1d**. In the absence of cod **4d** did not form even under refluxing conditions. For similar exchange processes at Pd⁰, see: G. T. L. Broadwood-Strong, P. A. Chaloner, P. B. Hitchcock, *Polyhedron* 1993, 12, 721.
- [18] P. E. Garrou, *Chem. Rev.* 1981, 81, 229.
- [19] J. G. Verkade, J. A. Mosbo, in *Phosphorus-31 NMR Spectroscopy in Stereochemical Analysis* (Eds.: J. G. Verkade, L. D. Quin), VCH, Weinheim, 1987, p. 432.
- [20] a) R. Benn, A. Rufinska, *Angew. Chem.* 1986, 98, 851; *Angew. Chem. Int. Ed. Engl.* 1986, 25, 861; b) H. Mason, *Chem. Rev.* 1987, 87, 1299; c) B. E. Mann, in: *Transition Metal Nuclear Magnetic Resonance* (Ed.: P. S. Pregosin), Elsevier, Amsterdam, 1991, p. 177; d) M. Bühl, *Organometallics* 1997, 16, 261.
- [21] a) R. Benn, C. Brevard, *J. Am. Chem. Soc.* 1986, 108, 5622; b) R. Benn, A. Rufinska, *Magn. Reson. Chem.* 1988, 26, 895; c) C. J. Elsevier, J. M. Ernsting, W. G. J. de Lange, *J. Chem. Soc. Chem. Commun.* 1989, 585; d) D. Nanz, Doctoral Thesis, University of Zürich, 1993.

- [22] For recent examples, see : a) J. M. Ernsting, C. J. Elsevier, W. G. J. de Lange, K. Timmer, *Magn. Res. Chem.* **1991**, *29*, S118; b) B. R. Bender, M. Koller, D. Nanz, W. von Philipsborn, *J. Am. Chem. Soc.* **1993**, *115*, 5889; c) T. G. Cherkasova, Yu. S. Varshavsky, I. S. Podkorytov, L. V. Osetrova, *Rhodium Express* **1993**, *0*, 21; d) J.-J. Brunet, G. Codmenges, D. Neibecker, K. Philippot, L. Rosenberg, *Inorg. Chem.* **1994**, *33*, 6373; e) D. J. Law, G. Bigam, R. G. Cavell, *Can. J. Chem.* **1995**, *73*, 635; f) C. J. Elsevier, B. Kowall, H. Kragten, *Inorg. Chem.* **1995**, *34*, 4836; g) A. Boerner, A. Kless, J. Holz, W. Baumann, A. Tillack, R. Kadyrov, *J. Organomet. Chem.* **1995**, *490*, 213; h) A. Boerner, A. Kless, R. Kempe, D. Heller, J. Holz, W. Baumann, *Chem. Ber.* **1995**, *128*, 767; i) P. W. Jolly, G. Hopp, E. Passelaigne, W. von Philipsborn, personal communication.
- [23] a) W. A. Fordyce, G. A. Crosby, *Inorg. Chem.* **1982**, *21*, 1455; b) F. D. Lewis, G. D. Salvi, D. R. Kanis, M. A. Ratner, *ibid.* **1993**, *32*, 1251.
- [24] Crystallographic data of complex **2**: Empirical formula: $C_{13}H_{13}F_6O_2Rh$, color: orange, formula weight: $418.14 \text{ g mol}^{-1}$, crystal system: orthorhombic, crystal size: $0.42 \times 0.32 \times 0.22 \text{ mm}^3$, space group: *Pbca* (No. 61), $a = 17.602(2) \text{ \AA}$, $b = 16.542(2) \text{ \AA}$, $c = 20.321(3) \text{ \AA}$, $V = 5917(2) \text{ \AA}^3$, $T = 20(1) \text{ }^\circ\text{C}$, $\rho_{\text{calc}} = 1.88 \text{ g cm}^{-3}$, $Z = 16$, $\mu = 12.0 \text{ cm}^{-1}$, $\sin \theta_{\text{max}}/\lambda = 0.588$, $\text{MoK}\alpha$ radiation ($\lambda = 0.71069 \text{ \AA}$), total no. of reflections: 9822, no. of independent reflections: 6734, no. of observed reflections [$I \geq 2\sigma(I)$]: 4496, $R = 0.036$, $R_w = 0.086$, no. of parameters refined: 413, GOF: 1.020, residual electron density: 0.34 e \AA^{-3} . Crystallographic data (excluding structure factors) for the structure reported in this paper have been deposited with the Cambridge Crystallographic Data Centre as supplementary publication no. CCDC-405950. Copies of the data can be obtained free of charge on application to The Director, CCDC, 12 Union Road, Cambridge CB21EZ, UK (Fax: Int. code + (1223) 336-033; e-mail: deposit@chemcrs.cam.ac.uk).
- [25] A detailed description of the ligand **3o** and its coordination chemistry will be given elsewhere: R. B. Bedford, P. A. Chaloner, R. Fornika, P. B. Hitchcock, W. Leitner, in preparation.
- [26] P. A. Tucker, W. Scutcher, D. R. Russel, *Acta Crystallogr.* **1975**, *B31*, 592.
- [27] P. M. Anderson, L. H. Pignolet, *Inorg. Chem.* **1981**, *20*, 4101.
- [28] Strictly speaking, this is only true for square-planar complexes such as **1** since the electronic preferences of the d^8 metal centre are also important in defining the structure. However, these parameters are identical for all the complexes **1** under scrutiny. Although the actual structural basis (ideal P-Rh-P angle, etc.) may be different in other complexes, the relative variations should be comparable, as the same interactions can be expected to operate within the chelate ring.
- [29] M. C. Hall, B. T. Kilbourn, K. A. Taylor, *J. Chem. Soc. (A)* **1970**, 2540.
- [30] a) D. Cremer, J. A. Pople, *J. Am. Chem. Soc.* **1975**, *97*, 1354; b) D. Cremer, J. A. Pople, *ibid.*, 1358.
- [31] Note that unlike in a five-membered ring with identical edges, envelope structures do not possess C_5 symmetry in these complexes as this would require the rhodium atom to occupy an apical position and would result in severe 1,3 strain of the R groups at phosphorus. Accordingly, C_5 symmetry is not observed in statistical analysis of crystallographically characterized $\{[R_2P(CH_2)_2PR_2]M\}$ fragments: D. A. Morton, A. G. Orpen, *J. Chem. Soc. Dalton Trans.* **1992**, 641.
- [32] F. H. Allen, J. E. Davies, J. J. Galloy, O. Johnson, O. Kennard, C. F. Macrae, E. M. Mitchell, G. S. Mitchell, J. M. Smith, D. G. Watson, *J. Chem. Info. Comput. Sci.* **1991**, *31*, 187.
- [33] Steric repulsion of *cis*-PR₃ ligands is a well-known phenomenon in coordination chemistry. It is interesting to note in this context that the complex $\{[(\text{o-tolyl})_3P]_2Rh(\text{hfacac})\}$ is not formed in detectable quantities from **2** according to procedure **B** even in the presence of an excess of the monodentate ligand; C. Six, W. Leitner, unpublished results.
- [34] W. R. Cullen, T.-J. Kim, F. W. B. Einstein, T. Jones, *Organometallics* **1985**, *4*, 346.
- [35] M. Portnoy, D. Milstein, *Organometallics* **1993**, *12*, 1655.
- [36] a) B. R. James, D. Mahajan, *Isr. J. Chem.* **1977**, *15*, 214; b) R. G. Ball, B. R. James, D. Mahajan, J. Trotter, *Inorg. Chem.* **1981**, *20*, 254.
- [37] a) J. M. Brown, P. A. Chaloner, A. G. Kent, B. A. Murrer, P. N. Nicholson, D. Parker, P. J. Sidebottom, *J. Organomet. Chem.* **1981**, *216*, 263; b) it is interesting to note that molecular mechanics, as described above and in ref. [9], predict a lowest energy conformation of the chelate ring in **3i** where one C-H bond is in close proximity to the metal atom and ideally aligned for oxidative addition.
- [38] N. F. Ramsey, *Phys. Rev.* **1950**, *78*, 699.
- [39] Extremely small P-Rh-P angles as encountered in four-membered chelate rings have a strong deshielding effect and lead to an increase in the chemical shift of the ^{103}Rh nucleus [22 a,f,i]. The special properties of four-membered chelates have been studied recently in detail by Hofmann and co-workers [3]. A full account of electronic and structural effects on the chemical shift of the ^{103}Rh nucleus in complexes of type **1** will be given separately. W. Baumann, M. Bühl, E. Dinjus, R. Fornika, M. Kessler, C. Krüger, W. Leitner, C. Six, in preparation.
- [40] a) M. Koller, W. von Philipsborn, *Organometallics* **1992**, *11*, 467; b) V. Tedesco, W. von Philipsborn, *ibid.* **1995**, *14*, 3600.
- [41] a) H. Bönemann, W. Brijoux, R. Brinkmann, W. Meurers, R. Mynott, W. von Philipsborn, T. Egolf, *J. Organomet. Chem.* **1984**, *272*, 231; b) H. Bönemann, *Angew. Chem.* **1985**, *97*, 264; *Angew. Chem. Int. Ed. Engl.* **1985**, *24*, 248.
- [42] M. L. Connolly, *Science* **1983**, *221*, 709.
- [43] Of course, this is a highly simplified view, but it is clear that the major changes in the set of ligands presented here are related to changes in the coordination geometry of the fragments $[P_2Rh]$, and a separate treatment seems therefore justified. It should be noted, however, that electronic effects in catalytic reactions that were expected to be mainly sterically controlled have recently attracted much attention [44] and warrant further studies.
- [44] Some recent examples: a) E. J. Jacobsen, W. Zhang, M. L. Güler, *J. Am. Chem. Soc.* **1991**, *113*, 6703; b) T. V. RajanBabu, T. A. Ayers, A. L. Casalnuovo, *ibid.* **1994**, *116*, 4101; c) A. L. Casalnuovo, T. V. RajanBabu, T. A. Ayers, T. H. Warren, *ibid.* 9869; d) A. S. C. Chan, C.-C. Pai, T.-K. Yang, S.-M. Chen, *J. Chem. Soc. Chem. Commun.* **1995**, 2031; e) S.-B. Park, K. Murata, H. Matsumoto, H. Nishiyama, *Tetrahedron Asymmetry* **1995**, *6*, 2487.
- [45] P. Margl, T. Ziegler, P. E. Blöchl, *J. Am. Chem. Soc.* **1995**, *117*, 12625.
- [46] a) K. Issleib, D.-W. Müller, *Chem. Ber.* **1959**, *92*, 1397; b) R. J. Burt, J. Chatt, W. Hussein, G. J. Leigh, *J. Organomet. Chem.* **1979**, *182*, 203; c) H. Brunner, H.-J. Lautenschlager, *Synthesis* **1989**, 706; d) E. Dinjus, W. Leitner, *Appl. Organomet. Chem.* **1995**, *9*, 43.
- [47] A. Bax, R. H. Griffey, B. L. Hawkins, *J. Magn. Reson.* **1983**, *55*, 301.